[9] Y. L. Chow, J. J. Yang, D. G. Fang, and G. E. Howard, "A closed-form spatial Green's function for the thick microstrip substrate," *IEEE Trans. Microw. Theory Tech.*, vol. 39, no. 3, pp. 588–592, Mar. 1991.
[10] M. I. Aksun and R. Mittra, "Derivation of closed-form Green's functions for a general microstrip geometry," *IEEE Trans. Microw. Theory Tech.*, vol. 40, no. 11, pp. 2055–2062, Nov. 1992.
[11] R. A. Kipp, C. H. Chan, A. T. Yang, and J. T. Yao, "Simulation of high frequency integrated circuits incorporating full wave analysis of microstrip discontinuities," *IEEE Trans. Microw. Theory Tech.*, vol. 41, no. 5, pp. 848–854, May 1993.
[12] R. A. Kipp and C. H. Chan, "Complex image method for sources in bounded regions of multilayer structures," *IEEE Trans. Microw. Theory Tech.*, vol. 42, no. 5, pp. 860–865, May 1994.
[13] C. H. Chan and R. A. Kipp, "Application of the complex image method to multilevel, multiconductor microstrip lines," *Int. J. Microw. Millimeter-Wave Comput.-Aided Eng.*, vol. 7, no. 5, pp. 359–367, 1997.
[14] F. Ling and J. M. Jin, "Discrete complex image method for Green's functions of general multilayer media," *IEEE Trans. Microw. Guided Wave Lett.*, vol. 10, no. 10, pp. 400–402, Oct. 2000.
[15] N. V. Shuley, R. R. Boix, F. Medina, and M. Horno, "On the fast approximation of Green's functions in MPIE formulations for planar layered media," *IEEE Trans. Microw. Theory Tech.*, vol. 50, no. 9, pp. 2185–2192, Sep. 2002.
[16] S.-A. Teo, S.-T. Chew, and M.-S. Leong, "Error analysis of the discrete complex image method and pole extraction," *IEEE Trans. Microw. Theory Tech.*, vol. 51, no. 2, pp. 406–413, Feb. 2003.
[17] M. I. Aksun, "A robust approach for the derivation of closed-form Green's functions," *IEEE Trans. Microw. Theory Tech.*, vol. 44, pp. 651–658, May 1996.
[18] A. Alparslan, M. I. Aksun, and K. A. Michalski, "Closed-form Green's functions in planar layered media for all ranges and materials," *IEEE Trans. Microw. Theory Tech.*, vol. 58, no. 3, pp. 602–613, Mar. 2010.
[19] V. I. Okhmatovski and A. C. Cangellaris, "A new technique for the derivation of closed-form electromagnetic Green's functions for unbounded planar layered media," *IEEE Trans. Antennas Propag.*, vol. 50, no. 7, pp. 1005–1016, Jul. 2002.
[20] F. Mesa, R. R. Boix, and F. Medina, "Closed-form expressions of multilayered planar Green's functions that account for the continuous spectrum in the far field," *IEEE Trans. Microw. Theory Tech.*, vol. 56, no. 7, pp. 1601–1614, Jul. 2008.
[21] R. R. Boix, A. L. Fructos, and F. Medina, "Closed-form uniform asymptotic expansions of Green's functions in layered media," *IEEE Trans. Antennas Propag.*, vol. 58, no. 9, pp. 2934–2945, Sep. 2010.
[22] Y. Hua and T. K. Sarkar, "Generalized pencil-of-function method for extracting poles of an EM system from its transient response," *IEEE Trans. Antennas Propag.*, vol. 37, no. 2, pp. 229–234, Feb. 1989.
[23] W. C. Chew, *Waves and Fields in Inhomogeneous Media*. New York, NY, USA: Van Nostrand Reinhold, 1990.

A Compact Wideband Slot-Loop Hybrid Antenna With a Monopole Feed

Guoping Pan, Yue Li, Zhijun Zhang, and Zhenghe Feng

***Abstract*—This communication presents a compact monopole-fed slot-loop hybrid antenna for wideband wireless communications. The wideband characteristic is achieved by coupling three different resonant modes of the proposed slot-loop hybrid antenna, namely, a loop mode for the lower band, a slot mode for the middle band and a monopole mode for the higher band. The proposed antenna is built and tested to verify the design strategy. The measured impedance bandwidth ($|S_{11}| < -10$ dB) ranges from 1.82 GHz to 5.68 GHz (102.9%) with stable performance, including bi-directional radiation pattern, vertical polarization and gain. The proposed slot-loop hybrid antenna also shows the merits of compact dimension, low cross-polarization and low cost.**

***Index Terms*—Loop antenna, multiple resonant modes, slot antenna, wideband antenna.**

I. Introduction

With the rapid advancement of modern wireless communication technology, there has been a great demand for wideband antennas in recent years. Good impedance match and reasonably stable radiation patterns in the band of the interest are the basic desired characteristics of the wideband antennas.

Different types of wideband planar antenna structures were reported in the literature [1]–[3]. In [1], a reconfigurable multi-band and wideband patch antenna employing dual-patch elements and C-Slots was reported, and the wideband mode with an impedance bandwidth of 33.52% could be obtained. In a study by S. I. Latif, *et al.* in [2], a monopole slot at the center of the ground plane was studied for its impedance bandwidth, with an obtained bandwidth of design of about 52.8%. A novel Ψ-shape microstrip patch antenna was reported in [3], with a measured 2:1 VSWR impedance bandwidth of 54%. Because of many advantages, such as low profile, ease of fabrication, and wide bandwidth, wide slot antennas have become the hot and focal point of wideband antenna research. To reduce the sizes and attain wider bandwidths, some printed wide slot antennas were extensively researched in [4]–[8]. In [4], a dual-polarization coplanar waveguide-fed slot antenna was proposed, and the -10-dB reflection coefficient bandwidths of two

Manuscript received January 26, 2013; revised April 16, 2014; accepted April 22, 2014. Date of publication April 29, 2014; date of current version July 02, 2014. This work was supported in part by the China Postdoctoral Science Foundation funded project 2013M530046, by the National High Technology Research and Development Program of China (863 Program) under Contract 2011AA010202, by the National Natural Science Foundation of China under Contract 61301001, and in part by the National Science and Technology Major Project of the Ministry of Science and Technology of China under Contract 2013ZX03003008-002.

G. Pan is with State Key Laboratory on Microwave and Digital Communications, Tsinghua National Laboratory for Information Science and Technology, Department of Electronic Engineering, Tsinghua University, Beijing 100084, China and also with China Satellite Maritime Tracking and Control Department, Jiangyin 214431, China.

Y. Li, Z. Zhang, and Z. Feng are with State Key Laboratory on Microwave and Digital Communications, Tsinghua National Laboratory for Information Science and Technology, Department of Electronic Engineering, Tsinghua University, Beijing 100084, China (e-mail: hardy_723@163.com).

Color versions of one or more of the figures in this communication are available online at http://ieeexplore.ieee.org.

Digital Object Identifier 10.1109/TAP.2014.2320535

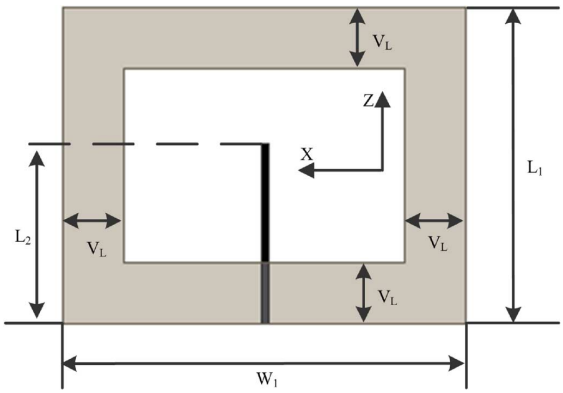

Fig. 1. Geometry and dimensions of the proposed antenna (the front side in gray color and the backside in black color).

polarizations were 27.9% for one polarization and 35.4% for the other. A printed wide slot antenna fed by a microstrip line with a fork-like tuning stub was proposed in [5], with a 1:1.5 VSWR bandwidth ranging from 1.821 GHz to 2.912 GHz. In [6], a microstrip-line-fed printed wide slot antenna with a fractal shaped slot for bandwidth enhancement was provided, and it could reach an operating bandwidth of 62.3%. For bandwidth enhancement, a printed wide slot antenna composed of an E-shaped slot on the ground plane excited by an E-shaped patch was designed in [7]. It had a wide operating bandwidth of over 120% (2.8–11.4 GHz) for $|S_{11}| < -10$ dB with the size of 85×85 mm^2. Sung studied a wide slot antenna with the square slot excited by an L-shaped microstrip line-fed consisting of a horizontal line, a square patch, and a vertical line [8]. It also had a wide impedance bandwidth of 118.4% for $|S_{11}| < -10$ dB with the size of 80×54 mm^2.

For the wideband antenna, it is important to stabilize the radiation patterns over the whole operating band. With the electric size varying large, the radiation patterns could be distorted seriously in wide band, thus how to keep the radiation pattern stable is a challenge in wideband antenna design. Some wideband antennas had achieved large impedance bandwidth in the literatures [9]–[12], but the available bandwidth of antennas of these wideband antennas were often limited by their distorted radiation pattern in spite of its large impedance bandwidth. To achieve large impedance bandwidth with stable radiation patterns, Quan Xue *et al.* placed a circular ring within the cavity between the bowtie and the ground plane to stabilize the radiation patterns [13].

This communication proposes a compact monopole-fed slot-loop wideband antenna with a stable radiation pattern and polarization. Compared with the designs in [5]–[12], the geometrical structure of the proposed antenna is quite simple, but the working principle is different. The wideband characteristic is achieved by coupling three different resonant modes of the proposed slot-loop hybrid antenna, namely, a loop mode, a slot mode and a monopole mode. The current and electric field distributions are analyzed at three different resonant modes. The measured impedance bandwidth for $|S_{11}| < -10$ dB is 3.86 GHz (102.9%), and the radiation patterns and gain performance of the proposed antenna are measured and compared with the simulation results.

II. Antenna Configuration and Design

Fig. 1 shows the geometry of the proposed slot-loop hybrid planar antenna. The antenna consists of a rectangular loop etched on the front side of a substrate and a monopole printed on the back side.

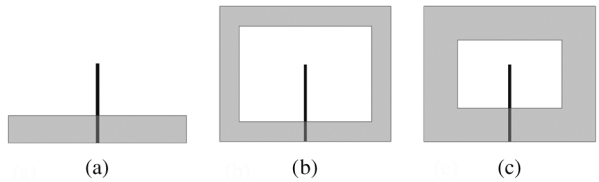

Fig. 2. Geometry of the monopole, the loop antenna, the slot antenna and the proposed antenna (the front side in gray color and the backside in black color); (a) the monopole antenna; (b) the loop antenna; (c) the slot antenna.

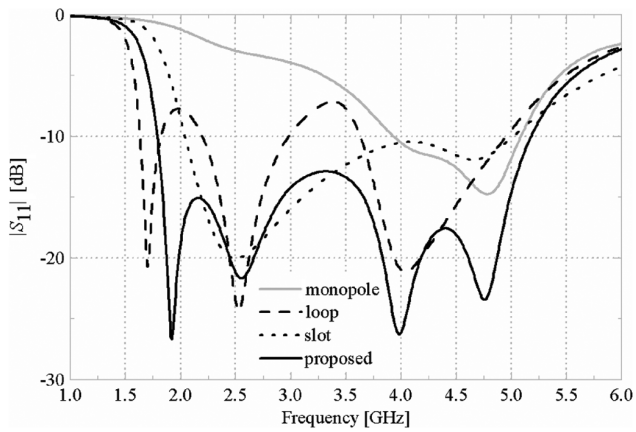

Fig. 3. Simulated reflection coefficients of the monopole, the loop antenna, the slot antenna and the proposed antenna.

The 1.6-mm-thick FR4 substrate size is $L_1 \times W_1$, which has a relative permittivity of 4.4 and a loss tangent of 0.02. The width of the loop is uniform and is defined as V_L. The length of the monopole is L_2 and the width is 1 mm. By optimizing the dimensions of the proposed antenna, the energy could be radiated mainly from the loop, the slot and the monopole at different frequency bands. What's more, the radiation patterns of the loop, the slot and the monopole are nearly similar when working at basic mode. Therefore, the wideband characteristic is achieved by coupling three different resonant modes of the proposed slot-loophybrid antenna, namely, a loop mode for the lower band, a slot mode for the middle band and a monopole mode for the higher band. And the radiation patterns could be stable at the whole band.

The design process of the proposed antenna is presented first. Fig. 2 shows the geometries of the monopole antenna, the loop antenna and the slot antenna, and all the FR4 substrate sizes and the lengths of the monopoles of these antennas are the same. The software Ansoft High Frequency Structure Simulator (HFSS) is used to simulate these antennas. Fig. 3 presents the simulated reflection coefficients of these antennas. For the monopole antenna, the central frequency is 4.78 GHz. For the loop antenna, the impedance bandwidth for $|S_{11}| < -10$ dB ranges from 1.63 GHz to 1.82 GHz, 2.2 GHz to 2.98 GHz, and from 3.63 GHz to 4.95 GHz. For the slot antenna, the impedance bandwidth for $|S_{11}| < -10$ dB ranges from 2.04 GHz to 5.01 GHz. To largely expand the impedance bandwidth, we could adjust the parameter, and design a monopole-fed slot-loop hybrid antenna. So, there are different working modes at different frequency bands. As a consequence, wider impedance bandwidth is achieved.

HFSS is also used for the parameter optimization. Fig. 4 presents the simulated reflection coefficient of the proposed antenna with different V_L. The lowest resonant frequency is observed to become

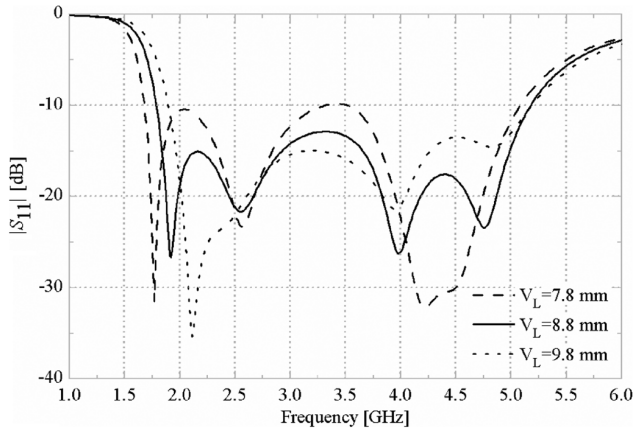

Fig. 4. Simulated reflection coefficients of the proposed antenna with different V_{L}.

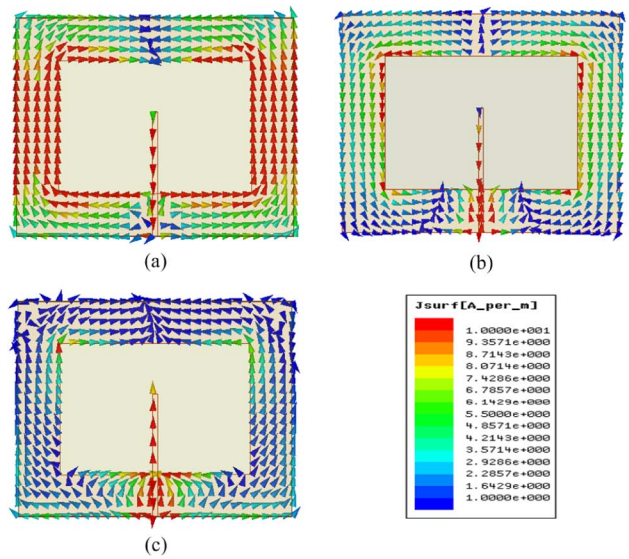

Fig. 5. Current distributions of the proposed antenna at: (a) 2 GHz; (b) 3 GHz; (c) 4.76 GHz.

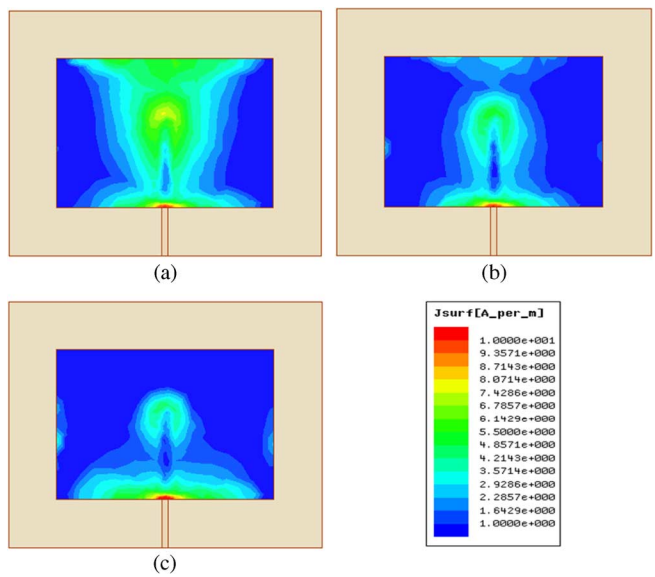

Fig. 6. Electric field distributions in slot at: (a) 2 GHz; (b) 3 GHz; (c) 4.76 GHz.

higher as the width V_{L} increases. When the width of V_{L} is 8.8 mm, the impedance matching properties of the proposed antenna are the best. Other parameters can also be optimized for better matching performance. The optimized parameters of the proposed antenna are: $L_1 = 45$ mm, $W_1 = 57.4$ mm, $V_{\mathrm{L}} = 8.8$ mm, and $L_2 = 25.6$ mm. The simulated reflection coefficients of the proposed antenna is shown in Fig. 3.

For the slot mode, the length of the slot is approximately half a wavelength. The width of the extended ground is a quarter-wavelength or smaller. As shown in Fig. 1, the resonance frequency is mainly determined by the width of $(W_1 - 2V_{\mathrm{L}})$, which also affects the coupling between the monopole and the loop. A loop antenna typically works at one-wavelength mode, and the loop has four edges with the total length of one wavelength. After optimizing the width of slot, we tune the value of L_1 to make sure that the loop operates in the one-wavelength mode. The monopole is not only used for feeding of the slot-loop hybrid antenna, but also radiates energy. In other words, for the slot mode, the current on the monopole is strong to produce coupling between the slot and the monopole. So, the monopole is mainly used to be coupling energy, and the slot is the main radiated element. The energy could be coupled from the monopole to the slot and radiated mainly from the slot. For the loop mode, the rest can be deduced by analogy. For the monopole mode, the monopole is the main radiator. For this mode, the length of the monopole is a quarter of wavelength. L_2 determines the operating frequency of the monopole. What should be mentioned is that for whatever mode, the relevant radiator is the main radiator, and the others also make a little contribution to the characteristics of the proposed antenna. Fig. 5 shows the current distributions of the proposed antenna at 2 GHz, 3 GHz and 4.76 GHz to study the coupling of the three modes. Fig. 5(a) shows the first resonant mode. A loop antenna typically works at one-wavelength mode, with the current distribution is mainly concentrated at the edges of the loop. Fig. 5(b) presents the second resonance mode. The wide slot width is approximately half a wavelength. The current distribution is mainly concentrated at the surrounds of the slot. Fig. 5(c) shows the third resonance mode. The length of the monopole is $\lambda/4$ (λ is the resonance wavelength), and the current distribution is mainly concentrated at the monopole. And there is few current on the loop. We also analyze the coupling of the three modes by using the electric field distributions. Fig. 6 shows the electric field distributions in the slot of the proposed antenna at 2 GHz, 3 GHz and 4.76 GHz. Fig. 6(a) shows the electric field distribution of the loop mode. The energy is coupled from the monopole to the loop. Fig. 6(b) presents the electric field distribution of the slot mode. The energy is coupled from the monopole to the slot, and the intensity of the electric field is the strongest at the middle of the slot. Fig. 6(c) shows the electric field distribution of the monopole mode; and the electric field distribution is mainly concentrated on the monopole. Therefore, wide impedance bandwidth is achieved by coupling these three modes.

III. Experiment Results and Analysis

Experiments were conducted to verify the above design and simulation results. The photograph of the proposed antenna is shown in Fig. 7. A coaxial probe is used to feed the antenna. The inner conductor is soldered to the monopole, and the outer conductor is soldered to one edge of the loop. Fig. 8 illustrates the simulated and measured reflection coefficients. The measured results agree well with the simulated data. The simulated and measured -10-dB bandwidths of reflection coefficients

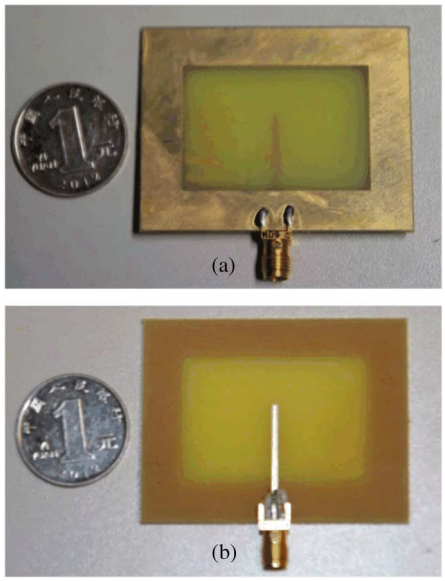

Fig. 7. Photograph of the proposed antenna: (a) front view; (b) back view.

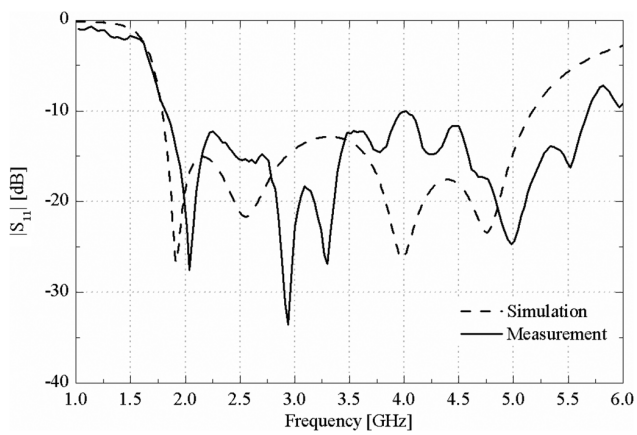

Fig. 8. Simulated and measured reflection coefficients of the proposed antenna.

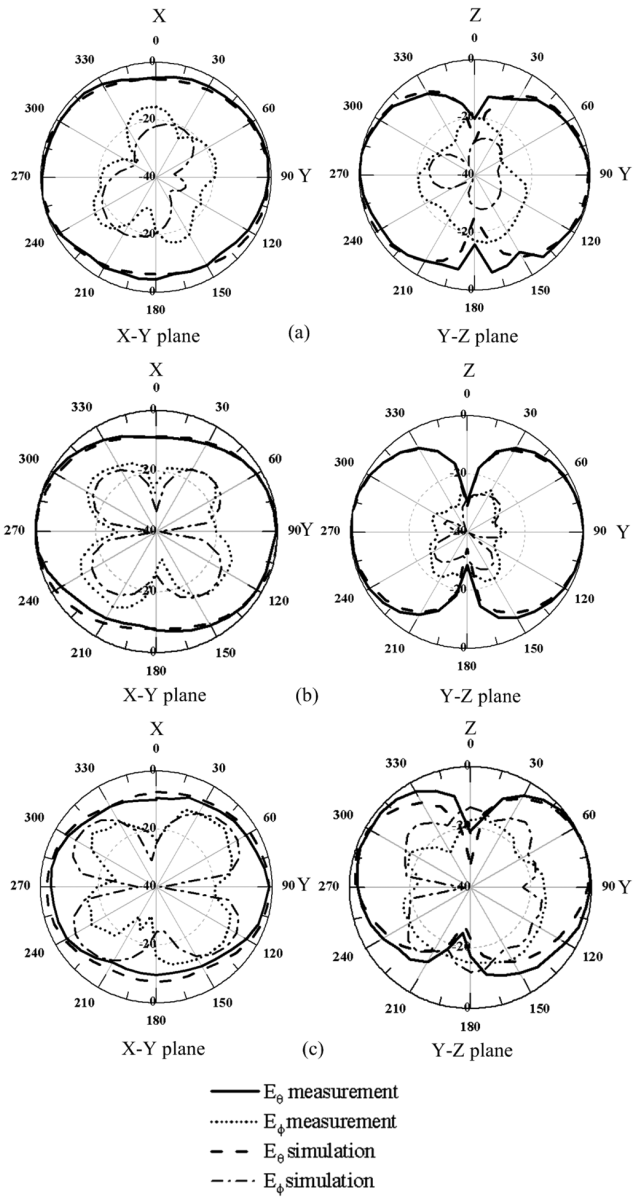

Fig. 9. The simulated and measured normalized radiation patterns of the proposed antenna: (a) 2 GHz; (b) 3 GHz; (c) 4.76 GHz.

are 3.38 GHz (1.79–5.17 GHz, 97.1%) and 3.86 GHz (1.82–5.68 GHz, 102.9%), respectively.

Fig. 9(a) to (c) show the simulated and measured normalized radiation patterns in the X-Y and the Y-Z planes of the proposed antenna at 2 GHz, 3 GHz and 4.76 GHz, respectively. Both the measured and the simulated co- and cross-polarization radiation patterns are similar and in good agreement. Radiation patterns at all these given frequencies are stably bi-directional. The vertical polarization is the dominant polarization. We define the 3-dB beamwidths at different frequencies to be the sums of 3-dB beamwidths in two different directions ($+$Y and $-$Y directions). The 3-dB beamwidths are both 180° in the H-plane (X-Y plane) and the E-plane (Y-Z plane) at 2 GHz, and cross-polarization levels are lower than 15 dB and 16.7 dB in the H- plane and the E-plane, respectively. The 3-dB beamwidths are 160° and 170° in the H-plane (X-Y plane) and the E-plane (Y-Z plane) at 3 GHz, and cross-polarization levels are lower than 11.32 dB and 21.5 dB in the H-plane and the E-plane, respectively. The 3-dB beamwidths are 110° and 130° in the H-plane (X-Y plane) and the E-plane (Y-Z plane) at 4.76 GHz, and cross-polarization levels are lower than 5.86 dB and 12.4 dB in the H-plane and the E-plane, respectively. It may be noted that the cross-polarization in the X-Y plane at 4.76 GHz is not as low as single monopole, because there are some strong transverse currents at the bottom edge of the loop, as can be seen in Fig. 5(c). From the radiation patterns in X-Y plane in Fig. 9(c), however, we notice that there appears to be a close correspondence between the minimum of E_{φ} and the maximum of the E_{θ}. Therefore, it is close to zero for the statistic integration of the two patterns. That is to say, the signals of the co-polarizations are irrelevant to those of the cross-polarizations. What's more, the cross-polarization levels are lower than 10.04 dB in 3-dB beamwidths in the X-Y plane at 4.76 GHz. The levels of cross polarization are much lower than those of co-polarization in 3-dB beamwidths in the X-Y and the Y-Z planes. Fig. 10 shows the measured and simulated gains of the proposed antenna. The measured gains fluctuate between 4.01 dBi and 5.3 dBi, and agree well with the simulated data. The differences between measurement and simulation are caused mainly by the loss of the substrate and the feeding cable.

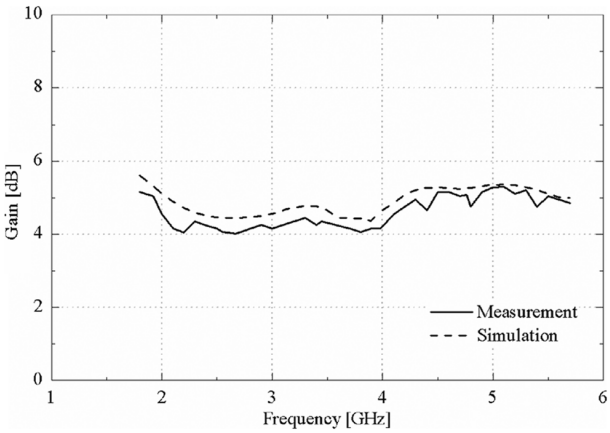

Fig. 10. Simulated and Measured gain of the proposed antenna.

TABLE I
THE BANDWIDTH COMPARISON OF THE PROPOSED ANTENNA WITH ANTENNA 1#–4#

antennas	bandwidth	Size (m^2)	R
Antenna 1#	46.1%	0.11×0.11	38.1
Antenna 2#	62.3%	0.07×0.07	127.1
Antenna 3#	120%	0.085×0.085	166.1
Antenna 4#	118.4%	0.08×0.054	274.1
The proposed antenna	102.9%	0.045×0.0574	398.4

The bandwidths of the presented antennas in [7] and [8] are better than that of the proposed antenna, but the size of the proposed antenna is 35.75% and 59.8% as large as the sizes of the presented antennas in [7] and in [8], respectively. Aiming to compare explicitly the bandwidth of the proposed antenna with those of the antennas presented in the literature [5]–[8], we define a value of $R = \mathrm{bandwidth/dimension}$, and name the antennas presented in [5]–[8] as antenna 1#, antenna 2#, antenna 3#, antenna 4#, respectively. A summary of the bandwidth comparison of the proposed antenna with the antenna 1# to antenna 4# is listed in Table I. The proposed antenna shows a better ratio of bandwidth and dimension than the reference antennas in [5]–[8].

IV. CONCLUSION

This communication presents a compact monopole-fed slot-loop hybrid antenna for wide impedance bandwidth. The structure of the proposed antenna is simple and compact, with the overall dimensions of $45 \times 57.4 \times 1.6\ \mathrm{mm}^3$. The wideband characteristic is achieved by coupling three different resonant modes of the proposed slot-loop hybrid antenna, namely, a loop mode, a slot mode and a monopole mode. The measured impedance bandwidth of $|S_{11}| < -10\ \mathrm{dB}$ is 3.86 GHz (1.82–5.68 GHz, 102.9%). Stable bi-directional radiation patterns, vertical polarizations and gain are observed in the overall band. The proposed antenna is a good candidate for a wideband wireless communication system.

REFERENCES

[1] H. F. AbuTarboush, R. Nilavalan, S. W. Cheung, K. M. Nasr, T. Peter, D. Budimir, and H. Al-Raweshidy, "A reconfigurable wideband and multiband antenna using dual-patch elements for compact wireless devices," *IEEE Trans. Antennas Propag.*, vol. 60, no. 1, pp. 36–43, Jan. 2012.

[2] S. I. Latif, S. K. Sharma, and L. Shafai, "Wideband microstrip monopole slot antenna," in *Proc. 6th Int. Symp. on Antennas, Propagation and EM Theory,* , Oct. 28–Nov. 1 2003, pp. 54–57.

[3] S. K. Sharma and L. Shafai, "A performance of a novel Ψ-shape microstrip patch antenna with wide bandwidth," *IEEE Antennas Wireless Propag. Lett.*, vol. 8, pp. 468–471, 2009.

[4] Y. Li, Z. Zhang, W. Chen, Z. Feng, and M. F. Iskander, "A dual-polarization slot antenna using a compact CPW feeding structure," *IEEE Antennas Wireless Propag. Lett.*, vol. 9, pp. 191–194, 2010.

[5] J. Y. Sze and K. L. Wong, "Bandwidth enhancement of a microstrip line-fed wide-slot antenna," *IEEE Trans. Antennas Propag.*, vol. 49, no. 7, pp. 1020–1024, Jul. 2001.

[6] W. L. Chen, G. M. Wang, and C. X. Zhang, "Bandwidth enhancement of a microstrip-line-fed printed wide-slot antenna with a fractal-shaped slot," *IEEE Trans. Antennas Propag.*, vol. 57, pp. 2176–2179, July 2003.

[7] A. Dastranj, A. Imani, and M. Naser-Moghaddasi, "Printed wide-slot antenna for wideband application," *IEEE Trans. Antennas Propag.*, vol. 56, no. 10, pp. 3097–3102, Oct. 2008.

[8] Y. Sung, "A printed wide-slot antenna with a modified L-shaped microstrip line for wideband applications," *IEEE Trans. Antennas Propag.*, vol. 59, no. 10, pp. 3918–3922, Oct. 2011.

[9] P. Li, J. Liang, and X. Chen, "Study of printed elliptical/circular slot antenna for ultrawideband applications," *IEEE Trans. Antennas Propag.*, vol. 54, no. 6, pp. 1670–1675, July 2006.

[10] G. Marchais, L. Ray, and A. Sharaiha, "Stripline slot antenna for UWB communications," *IEEE Antennas Wireless Propag. Lett.*, vol. 5, pp. 319–322, 2006.

[11] S. W. Qu, C. L. Ruan, and B. Z. Wang, "Bandwidth enhancement of wide-slot antenna fed by CPW and microstrip line," *IEEE Antennas Wireless Propag. Lett.*, vol. 5, pp. 15–17, 2006.

[12] L. Li, J. Yang, X. Chen, X. Zhang, R. Ma, and W. Zhang, "Ultrawideband differential wide-slot antenna with improved radiation patterns and gain," *IEEE Trans. Antennas Propag.*, vol. 60, no. 12, pp. 6013–6018, Dec. 2012.

[13] S.-W. Qu, J.-L. Li, Q. Xue, and C. H. Chan, "Wideband cavity-backed bowtie antenna," *IEEE Trans. Antennas Propag.*, vol. 56, no. 12, pp. 3850–3854, Dec. 2012.